Particulate biogenic barium tracer of mesopelagic carbon remineralization in the Mediterranean Sea (PEACETIME project)

Stéphanie H.M. Jacquet[1*], Christian Tamburini[1], Marc Garel[1], Aurélie Dufour[1], France VanVambeke[1], Frédéric A.C. Le Moigne[1], Nagib Bhairy[1], Sophie Guasco[1]

[1]Aix Marseille Université, CNRS/INSU, Université de Toulon, IRD, Mediterranean Institute of Oceanography (MIO), UM 110, 13288 Marseille, France

[*]Correspondence to: S. Jacquet (*stephanie.jacquet@mio.osupytheas.fr)*

PEACETIME special issue

ABSTRACT

We report on the sub-basins variability of particulate organic carbon (POC) remineralization in the western and central Mediterranean Sea during a late spring period (PEACETIME cruise). POC remineralization rates were estimated using the excess biogenic particulate barium (Ba_{xs}) inventories in mesopelagic waters (100-1000 m) and compared with prokaryotic heterotrophic production (PHP). Ba_{xs}-based mesopelagic remineralization rates (MR) range from 25 ± 2 to 306 ± 70 mg C m^{-2} d^{-1}. MR are larger in the Alger (ALG) basin compared to the Tyrrhenian (TYR) and Ionian (ION) basins. Our Ba_{xs} inventories and integrated PHP data also indicates that significant mesopelagic remineralization occurs down to 1000 m depth in the ALG basin in contrast to the ION and TYR basins where remineralization is mainly located in the upper 500 m horizon. We proposed that the larger and deeper MR rates in the ALG basin would be sustained by an additional particles export event driven by deep convection. The ION basin (in contrast to the ALG and TYR basins) presents the impact of a previous dust event as reflected by our particulate Al water column concentrations. The ION and TYR basins are also the site of small-scale heterogeneity of stages of remineralization processes, as especially reflected by our Ba_{xs} inventories and integrated PHP data at the #Tyrr long duration station. This heterogeneity is linked to the mosaic of blooming and non-blooming patches reported in this area during the cruise. Contrastingly to the western Mediterranean Sea (ALG basin), the central Mediterranean Sea (ION and TYR basins) shows lower (intensity) and upper mesopelagic-layer restricted remineralization processes during the late spring PEACETIME cruise.

1. Introduction

In the ocean, remineralization rate associated with sinking particles is a crucial variable for air sea CO_2 balance [Kwon et al., 2009]. Most of the sinking particulate organic carbon (POC) conversion (i.e. remineralization) into CO_2 by heterotrophic organisms (i.e. respiration) occurs within the mesopelagic zone (100-1000 m) [Martin et al., 1987; Buesseler et al., 2007; Buesseler and Boyd, 2009]. A quantitative representation of this process is thus crucial to future predictions of the ocean's role in the global C cycle [IPCC, 2014]. Particulate biogenic barium (Ba_{xs}) is a geochemical tracer of POC remineralization in the mesopelagic layer. Ba_{xs} occurs in the form of barite ($BaSO_4$ crystals) in the dark ocean as a byproduct of prokaryotic remineralization. In a global ocean undersaturated with respect to barite [Monnin and Cividini, 2006], Ba_{xs} precipitates inside oversaturated biogenic micro-environments during POC degradation by heterotrophic prokaryotes, through sulfate and/or barium enrichment [Dehairs et al., 1980; Stroobant et al., 1991; Bertram and Cowen, 1997; Ganeshram et al., 2003]. By applying a transfer function relating Ba_{xs} to O_2 consumption [Dehairs et al., 1997] Ba_{xs} has been widely used since the 90's as an estimator of mesopelagic POC remineralization rates in various sectors of the Southern Ocean, North Pacific and North Atlantic [Cardinal et al., 2001, 2005; Dehairs et al., 2008; Jacquet et al., 2008a, 2008b, 2011, 2015; Planchon et al., 2013; Lemaitre et al., 2018]. Jacquet et al. [2021] recently reported that such transfer function could be applied in the Mediterranean Sea without restriction. This last study complemented previous investigations aiming at improving the use of Ba_{xs} to estimate local processes of POC remineralization in the Mediterranean Sea [Jacquet et al., 2016; Jullion et al., 2017]. In this prospect, the Mediterranean Sea represents a unique case study, mainly due to unresolved issues related to the imbalance in the regional C budget such as the coupling between surface biology and deeper remineralization, timescales of their variability between basins and discrepancies between mesopelagic trophic regime and respiration dynamics [Sternberg et al., 2007, 2008; Santinelli et al., 2010; Lopez-Sandoval et al., 2011; Luna et al., 2012; Tanhua et al., 2013b; Malanotte-Rissoli et al., 2014].

The present work is part of the PEACETIME project (ProcEss studies at the Air-sEa Interface after dust deposition in the MEditerranean sea) (http://peacetime-project.org/). PEACETIME aimed at studying the impact of atmospheric Saharan dust on the Mediterranean biogeochemistry [Guieu et al., 2020a]. Dust deposition is a major source of macro and micro nutrients and ballasted material to surface waters that likely impacts the biological carbon pump through organic matter production (i.e. primary production) and its subsequent export and remineralization in the water column [Pabortsava et al., 2017; Gazeau et al., 2021]. Overall, the aims of the present contribution to the PEACTIME project were: (1) to document particulate biogenic Ba_{xs} in different ecoregions of the western and central parts of the Mediterranean Sea. Previous Ba_{xs} data in the Mediterranean Sea are relatively scarce with limited vertical sampling resolution [Sanchez-Vidal et al., 2005] or restricted locations [Dehairs et al., 1987; Sternberg et al., 2007, 2008; van Beek et al., 2009]; (2) to determine the relationship between Ba_{xs} and environmental variability, including dust deposition, (3) to estimate Ba_{xs}-based POC remineralization rates (MR) at mesopelagic depths according to the Dehairs' transfer function [Dehairs et al., 1997] we have recently validated for the Mediterranean Sea [Jacquet et al., 2021], and (4) assess potential differences in remineralization length scale of POC in the various ecoregions of the Mediterranean Sea.

Code de champ modifié

2. Material and methods

2.1 Study area

The PEACETIME cruise (https://doi.org/10.17600/17000300) was conducted during late spring conditions from May 10 to June 11, 2017 (French R/V Pourquoi pas?) in the western and central Mediterranean (Figure 1a). The Mediterranean Sea is a semi-landlocked sea with limited, but crucial, exchange with the Atlantic Ocean, two deep overturning cells, one shallow circulation and a complex upper layer circulation with several permanent and quasi-permanent eddies. The Mediterranean Sea is furthermore characterized by contrasting ecosystems, from strongly oligotrophic deep interiors to eutrophic Adriatic [Durrieu de madron et al., 2011; Reygondeau et al., 2017]. The studied zone crossed the typical eastward increasing oligotrophic trend as reported in previous studies [Moutin and Raimbault, 2002; Pujo-Pay et al., 2011; Tanhua et al., 2013a; Guieu et al., 2020a]. However, this trend was not homogeneous, as for instance in the Ionian Sea (a crossroad of waters of contrasted biological history) where blooming and non-blooming mosaic areas co-occur in spring [Berline et al., 2021].

The hydrography during the PEACETIME cruise displayed the general three-layer Mediterranean system with surface, intermediate and deep waters [Tamburini et al., 2013; Tanhua et al., 2013a; Hainbucher et al., 2014, Malanotte-Rizzoli et al., 2014]. Briefly, the main water masses can be distinguished (see potential temperature – salinity diagram in Figure 1b): (1) from west to east surface Atlantic Water (SW) is gradually replaced by Ionian surface Water (ISW) and Levantine Surface water (LSW); (2) Winter Intermediate Water (WIW) and Levantine Intermediate water (LIW). LIW is present at intermediate depths (from 200 to 800 m) and is characterized by a local maximum of salinity and a local minimum of dissolved oxygen concentration; (4) Mediterranean Deep Water (MDW).

Three main ecoregions [Reygondeau et al., 2017; Ayata et al., 2018] were crossed during the cruise: the Algero-Provençal basin (later referred to as ALG), the Tyrrhenian basin (TYR) and the Ionian basin (ION) (Figure 1a).

2.2 Barium sampling and sample processing

Thirteen stations were sampled for particulate barium from surface to 2000 m (thirty depths in total) in the ALG (stations #1, #2, #3, #10, #Fast, #9 and #4), TYR (stations #5, Tyrr and

#6) and ION (stations #8, #7 and #Ion) basins (Table 1). Three of these stations were sampled twice on different days (long duration stations #Fast, #Tyrr and #Ion), but due to technical problem no particulate barium data are available for the second visit at station #Ion. Three days separate both visits at station #Fast and two days at #Tyrr.

For particulate barium, 4 to 6 L of seawater sampled using Niskin bottles were filtered onto 47 mm polycarbonate membranes (0.4 µm porosity) under slight overpressure supplied by filtered air. Filters were rinsed with few mL of MQ water grade to remove sea salt, dried (50°C) and stored in Petri dishes for later analysis. In the laboratory, we performed a total digestion of filters using a concentrated tri-acid (0.5 mL HF /1.5 mL HNO_3 / HCl 1 mL; all Optima grade) mixture in closed teflon beakers overnight at 95°C in a clean pressurized room. After evaporation close to dryness, samples were re-dissolved into 10 mL of HNO_3 2%. The solutions were analysed for Ba and other elements of interest (i.e. Al, Na, Sr and Ca) by HR-ICP-MS (High Resolution-Inductively Coupled Plasma- Mass Spectrometry; ELEMENT XR, Thermo). Based on analyses of external certified reference standards, accuracy and reproducibility were both within ±5%. Details on sample processing and analysis are given in Cardinal et al. [2001] and Jacquet et al. [2015]. The presence of sea-salt was checked by analysing Na and the sea-salt particulate Ba contribution was found negligible (<0.1% of total Ba). Particulate biogenic barium in excess (hereafter referred to as Ba_{xs}) was calculated as the difference between total Ba and lithogenic Ba. The lithogenic Ba concentration was determined using Al concentration and the upper continental crust (UCC) Ba:Al molar ratio [Dymond et al., 1992; Taylor and Mc Lennan, 1985]. The standard uncertainty [Ellison et al., 2000] on Ba_{xs} concentration ranges between 5.0 and 5.5%. The term "in excess" is used to indicate that concentrations are larger than the Ba_{xs} background. The background (or residual value) is considered as "preformed" Ba_{xs} at zero oxygen consumption left over after transfer and partial dissolution of Ba_{xs} produced during degradation of previous particles export events. This background Ba_{xs} value likely depends on the saturation state of the water with respect to barite ($BaSO_4$, the main phase of particulate biogenic barium). Saturation indexes were reported in Jacquet et al. [2016] over a high resolution and quasi-zonal Mediterranean transect (M84/3 cruise; Tanhua et al., 2013a, 2013b). They revealed that the water column throughout the study area is largely undersaturated, with saturation state ranging between 0.2 and 0.6. A background Ba_{xs} value of 130 pM was recently reported in Jacquet et al. [2021]. It is close to the average Ba_{xs} contents observed at greater depth (>1000 m) in the present study (see below).

2.3 Prokaryotic heterotrophic production

Prokaryotic heterotrophic production (PHP) estimation was measured by incorporating L-[4,5-3H]-Leucine (^{3}H-Leu, specific activity 109 Ci mmol^{-1}, PerkinElmer®) technique (Kirchman, 1993). Details of the protocols can be found in Van Wambeke et al. (2021). Briefly, epipelagic layers (0-200 m) 1.5 ml volumes were incubated at 20 nM final concentrations and treated using the microcentrifuge technique. In Mesopelagic layers samples of 20 ml (200-800 m) and 40 ml (over 800 m) were incubated using 20 nM and 10 nM final Leucine concentration, respectively; and were treated using the filtration technique. Samples were incubated at in situ temperature. To calculate PHP, we used the empirical conversion factor of 1.5 ng C per pmol of incorporated leucine assuming that, isotopic dilution was negligible under saturating concentrations of leucine as, this was checked occasionally with concentration kinetics.

2.4 POC remineralization rates

We recently reported on the validity of the Dehairs's transfer function [Dehairs et al., 1997] in the Mediterranean basin to estimate mesopelagic POC remineralization [Jacquet et al., 2021]. We applied the similar approach to estimate remineralization rates (MR):

$$MR = [(Ba_{xs} - Ba\ BKG)/17450] \times Z \times RR \quad (Eq.1)$$

where Ba_{xs} is the depth-weighted average Ba_{xs} value (DWA; pM), i.e. the Ba_{xs} inventory divided by the depth layer considered Z, and RR the Redfield C/O_2 molar ratio (127/175; Broecker et al., 1985). As reported above, a Ba background (BKG) value of 130 pM was used. Volumetric MR rates were then integrated over the 100-500 m (upper mesopelagic zone) and 100-1000 m (entire mesopelagic zone) depth layers.

3. Results

Particulate biogenic Ba_{xs}, biogenic Ba fraction (%) and particulate Al, Sr and Ca concentrations are reported in Figure 2 in the upper 2000 m along a zonal transect crossing the three main sub-basins. PHP rates are also reported in Figure 2 in the upper 500 m along the same transect.

Ba_{xs} displays a similar water column distribution as reported in various sectors of the global Ocean, i.e. relatively low surface concentrations, a maximum in the mesopelagic layer (100-1000 m) followed by a decrease of concentrations back to a background level at deeper depths, usually 1000 m. At stations #9, #Tyrr, #8 and #Ion, Ba_{xs} concentrations in the upper 100 m are quite high (>5000 pM), with values reaching up to 11700 pM (80 m at station #Tyrr) (Figure 2a). Such high Ba_{xs} contents in the surface are quite unusual, though similar values (up to 9000 pM) were occasionally observed in earlier Southern Ocean studies [Dehairs et al., 1991, 1997; Jacquet et al., 2007b, 2008a, 2008b]. The high Ba_{xs} values at stations #Tyrr and #Ion are associated with higher Sr (up to 4267 pM at 100 m at station #Ion) and Ca (>130 nM) concentrations (Figure 2d, e). Thoughtout the water column, Sr and Ca concentrations range from to 448 to 6938 pM and from 30 to 488 nM, respectively. Sr/Ca molar ratios range from 7 to 45 mmol mol^{-1}, which is in the range of ratios reported in organic material [Martin and Knauer, 1976]. The upper mesopelagic layer (100-500 m) shows the characteristic Ba excess (maximum), as illustrated in Figure 3a. The lithogenic impact on the Ba_{xs} signal is relatively low (<20 %) except at stations #4, #5 and #Tyrr where it can reach up to 30 % at some depths in the water column (Figures 2b, 3b). The Ba_{xs} maximum at stations in the ALG basin and at station #7 in the ION basin presents a deeper extent compared to stations in the TYR basin (Figure 2a). At station #Ion Ba_{xs} maximum coincides with higher Ca (up to 186 nM) concentrations between 300 and 400 m (Figure 2e). However, the Ba_{xs} maximum is not restricted to the upper mesopelagic layer and also extents deeper. This is especially salient at stations in the ALG basin. At the other stations Ba_{xs} concentrations below 500 m decrease to reach the background value of around 130 pM. Among stations sampled twice for barium during the cruise, station #Fast (ALG basin) presents similar Ba_{xs} profiles except between 400 and 1000 m with lower concentrations measured during the second visit (3 days later; Figure 3a). The Ba_{xs} signal is mostly biogenic and rather stable over the whole water column at this station. It is also the case at station #Ion. In contrast, at station #Tyrr differences between Ba_{xs} profiles mainly occurred in the surface layer and upper mesopelagic layer, with relatively higher Ba_{xs} peaks during the second visit (2 days later). The biogenic Ba fraction at this station is also more variable throughout the water column.

PHP rates decrease from west to east in surface waters (Figure 2f). At station #Fast, PHP rates decreased from 49 ng C l^{-1} h^{-1} in surface to values between 7 and 11 ng C l^{-1} h^{-1} at 100 m depth and below 6 ng C l^{-1} h^{-1} below 200 m depth (Figure 3d). Same trend can be found in #Tyrr and #Ion stations with a rate in surface waters of around 36 and 25 ng C l^{-1} h^{-1} respectively (Figure 3e and 3f).

Depth-weighted average (DWA) concentrations of Ba_{xs} are reported in Table 1 for the upper (100-500 m) and entire (100-1000 m) mesopelagic layer. Since the base of the mixed layer was generally shallower than 100 m, this depth is taken as the upper boundary of the mesopelagic domain. DWA values range from 221 to 979 pM. On average stations located in the ALG basin present higher DWA than in the TYR and ION basins. DWA Ba_{xs} values remained rather stable over the 3–day period at station #Fast between 100 and 500 m, but displayed a decrease from 527 to 381 pM when considering the entire 100-1000 depth layer, corroborating above-mentioned profiles variation. In contrast, at station #Tyrr DWA Ba_{xs} values for the 100-500 m and 100-1000 m layers both increased over the 2–day period (from 284 to 542 pM and from 200 to 380 pM, respectively). On average DWA Ba_{xs} reached 577±286, 378±123 and 529±213 pM (100-500 m), and 527±288, 280±82 and 358±112 pM (100-1000 m) in the ALG, TYR and ION basin, respectively.

4. Discussion

4.1 Ba_{xs} distributions across the sub-basins

The very high Ba_{xs} concentrations reported in the surface layer at stations #9, #Tyrr, #8 and #Ion are associated with local Sr and Ca maxima, likely linked with potentially ballasted phytoplankton-derived material. Similar observations were previously reported in the Southern Ocean, revealing that in the surface water particulate Ba_{xs} is incorporated into or adsorbed onto biogenic material, with barite being a minor component [Dehairs et al., 1991, 1997; Jacquet et al., 2007a, 2008a, 2008b]. Below the surface layer, Ba_{xs} presents the characteristic maximum reflecting remineralization processes in the mesopelagic layer. Mesopelagic Ba_{xs} distributions are similar to those reported in Jacquet et al. [2021] and Sternberg et al. [2008] in the northwestern Mediterranean Sea (ANTARES and DYFAMED observatory sites, respectively). The Ba_{xs} maximum extents up to 1000 m in the ALG basin, while it is mostly located in the upper 500 m in the TYR basin. The lithogenic impact on the Ba_{xs} signal is globally relatively very low (<5%), except at stations #4, #5 and #Tyrr where it is more variable and can reach up to 30 % at some depths. A large dust deposition event occurred over a large area including the southern Tyrrhenian Sea just before the beginning of the PEACETIME campaign. Particulate Al concentrations and estimated lithogenic Ba fraction were sampled at these stations 5 to 12 days after the event and reflect an impact of this dust event in depth. Our conclusions are furthermore supported by results reported in

Bressac et al. [this issue]. These authors showed that Saharan dust depositions strongly impacted Stations #4, #5, #Tyrr and #6 and that significant fraction of dust particles was transferred to mesopelagic depths.

4.2 Mesopelagic Ba_{xs} and prokaryotic heterotrophic production

Previous studies highlighted the relationship between the mesopelagic Ba_{xs} and the vertical distribution of prokaryotic heterotrophic production (PHP), reflecting the temporal progression of POC remineralization processes. Mesopelagic Ba_{xs} content is indeed smaller when most of the column integrated PHP is restricted to the upper mixed layer (indicating an efficient, close to complete remineralization within the surface), compared to situations where a significant part of integrated PHP was located deeper in the water column (reflecting significant deep prokaryotic activity and POC export). Figure 3d-f shows PHP profiles in the upper 1000 m at long station #Fast, #Tyrr and #Ion. The whole dataset is discussed in VanWambeke et al. [2021]. Figure 4 shows column-integrated PHP at 100 m over column-integrated PHP at 500 m vs. DWA Ba_{xs} calculated over the 100-500 m depth interval. Results are confronted to the data obtained in the Southern Ocean [Jacquet et al., 2008a, 20015] and recently in the northeast Atlantic and northwestern Mediterranean Sea (PAP and ANTARES observatory sites, respectively) [Jacquet et al., 2021]. The blue line in Figure 4 represents the trend obtained during KEOPS2 [Jacquet et al., 2015]; it does not include encircled data points referred to as "season advancement". Results during PEACETIME follow the same trend, indicating higher DWA Ba_{xs} in situation where a significant part of column-integrated PHP is located deeper in the water column (high Int.PHP100/IntPHP500 ratio, Figure 4). Note that some data points, characterized by low DWA Ba_{xs} values, do not follow the trend from KEOPS2 (stations #3, #5 and #Tyrr2). During KEOPS2, the lowest DWA were reported for stations located in a meander and reflected the occurrence of different (earlier) stages of bloom advancement compared to the other stations (see "season advancement" in Figure 4).

Similarly, station #5 and #Tyrr2 would reflect evolution of the establishment (or advanced stages) of mesopelagic remineralization processes in the TYR basin compared to the other basins. Measurements performed during the second visit at station #Tyrr4 two days later corroborate this hypothesis and would reflect an increase of remineralization processes in the upper mesopelagic layer (DWV Ba_{xs} increased from 284 to 542 pM). At the DYFAMED station, Sternberg et al. [2008] reported the seasonal evolution of Ba_{xs} profiles on a monthly basis between February and June 2003. These authors showed the mesopelagic Ba_{xs} maximum builds up (and barite stock increase) following the spring phytoplankton bloom development, POC fluxes and subsequent remineralization processes. DWA Ba_{xs} reported in the present study are globally higher than those (maximum of 463 pM; 0-600 m) reported in Sternberg et al. [2008]. They also present a variability over the two days period at station #Tyrr of the same order of magnitude as reported over the season at DYFAMED. Furthermore, the increase of DWA Ba_{xs} at station #Tyrr is similar to those reported by Jacquet et al. [2007a; 2015] and Cardinal et al. [2005] over a few days to week period in different sectors of the Southern Ocean. Overall, the column-integrated PHP vs. DWA Ba_{xs} ratio we report at station #Tyrr confirms that the second repeat experienced higher remineralization processes in the upper mesopelagic layer than during the first occupation.

4.3 Mesopelagic C remineralization

We translated mesopelagic Ba_{xs} DWA into POC remineralization rates (MR) using Eq. (1). Figure 5 reports MR rates for the upper (100-500 m) and entire (100-1000 m) mesopelagic layer. MR range from 25 ± 2 to 306 ± 70 mg C m^{-2} d^{-1}. Primary production during the cruise ranged from 138 to 284 mg C m^{-2} d^{-1} [Figure 5; van Wambeke et al., 2021]. We observe a large difference in MR rates in the ALG basin depending on the integration depths. This is especially salient at station #9 with MR of 91 mg C m^{-2} d^{-1} in the upper mesopelagic layer and of 306 mg C m^{-2} d^{-1} in the entire mesopelagic layer (Figure 6). Results reveal significant remineralization occurred between 500 and 1000 m in the ALG basin. In contrast, in the ION and TYR basins MR rates reflect that remineralization is mainly located in the upper 500 m horizon. Similar conclusion was reported in a previous work of Jullion et al. [2017] reporting dissolved Ba and Parametric Optimum Multiparameter (POMP)-derived POC remineralization fluxes along a zonal transect between the Lebanon coast and Gibraltar (from 156 to 348 mg C m^{-2} d^{-1}; M84/3 cruise, April 2011). Independently of any dust consideration, these authors showed significant differences in the mesopelagic MR between the West and the East of the Mediterranean basin, suggesting an additional export pathway and subsequent remineralization driven by the winter deep convection in the western basin. The western basin is indeed the site of both shelf and open ocean deep convection, transferring biogeochemical components to the deep water such as inorganic and organic matter [Durrieu de Madron et al., 2013; Stabholz et al., 2013]. Following the hypothesis of particle injection pump [Boyd et al., 2019], the larger MR fluxes we report in the ALG basin during PEACETIME are in line with an ecoregion functioning within which recurrent transfer of material to depths by deep convection would sustain deeper mesopelagic remineralization processes. In contrast in the TYR basin remineralization appears mainly located in the upper mesopelagic layer. Stations in the TYR basin experienced a dust event and our particulate Al concentrations and estimated lithogenic Ba fraction reflect the impact of this event. At station #Tyrr the DAW Ba_{xs} vs. column-integrated PHP trend between the two visit reveals increasing MR rates mainly localized in the upper 500 m. Despite this increase, we can wonder whether the overall impact of the dust event would result in global lower (intensity) and upper mesopelagic layer-restricted MR processes. This would suggest that by providing ballast material (dust), and thereby decreasing of the exposition time of particles to prokaryotic remineralization [Pabortsava et al., 2017], the dust event reduced MR at station #Tyrr. Another dust event occurred on June 5 a few hours after the first sampling at station #Fast in the ALG basin.

However, station #Fast does not present any evidence of an impact at mesopelagic depths on particulate Al concentrations and estimated lithogenic Ba fraction. It is obvious that the time laps between the dust event and our sampling was too short (in contrast to station #Tyrr where the dust event occurred 5 to 12 days before). In contrast to variables change in the surface layer, observable response in the establishment of the biological C pump (towards mesopelagic remineralization and subsequent Ba_{xs} formation) to a single dust event would require more time. Regarding the ION basin, while stations do not reflect the impact of any dust event (as reported in the TYR basin) and are not subject to potential deep convection (as reported in the ALG basin), DWA Ba_{xs} and MR fluxes are also restricted to the upper mesopelagic layer. In Berline et al. [this issue] authors report the small-scale heterogeneity of particles abundance at ION stations, emphasizing the spatial decoupling between particle production and particle distribution and adding complexity in assessing time lag between production and export of particles, and thus C transfer efficiency [Stange et al., 2017; Henson et al., 2011]. Especially, Berline et al. [this issue] report the absence of significant surface production event in this basin. They also report for instance that surface particles at station #8 relate to a past production event that has not been exported yet. As reported in Van Wambeke et al. [this issue] primary production fluxes were slightly higher in the ION basin (from 158 to 208 mg C m^{-2} d^{-1}) than in the TYR basin (from 142 to 170 mg C m^{-2} d^{-1}). Overall, DWA Ba_{xs} and MR fluxes reported in the ION basin would thus reflect earlier stage of remineralization processes. The same conclusion stands for station #Tyrr 2 (in contrast to #Tyrr4) according to the DWA Ba_{xs} vs integrated-PHP trend.

5. Conclusion

The present paper presents an expended dataset on the Ba_{xs} distribution in the ALG, TYR and ION basins (western and central Mediterranean Sea) in late spring 2017. Results highlight that mesopelagic remineralization processes are mainly located in the upper 500 m horizon in the TYR and ION basins, while they occur in the lower mesopelagic zone (down to 1000 m) in the ALG basin. We suggest that the particle injection pump driven by recurrent and strong deep convection in the western basin would sustain the larger and deeper MR rates we observe in the ALG basin. Regarding both TYR and ION basins, it is difficult to figure out whether it is the impact of a previous dust event or the pactchiness of time lags between production and export of particles which resulted in lower (intensity) and upper mesopelagic-layer restricted remineralization processes.

Data availability

Underlying research data are being used by researcher participants of the PEACETIME campaign to prepare other papers, and therefore data are not publicly accessible at the time of publication. The Guieu et al. (2020b) study will be accessible at https://www.seanoe.org/data/00645/75747/, once the special issue is completed (all papers should be published by June 2021).

Author contributions

SJ wrote the manuscript with the contribution of all co-authors.

Competing interests

The authors declare that they have no known competing financial interests or personal relationships that could have appeared to influence the work reported in this paper.

Special issue statement

This article is part of the special issue “Atmospheric deposition in the low-nutrient–low-chlorophyll (LNLC) ocean: effects on marine life today and in the future (ACP/BG interjournal SI)”. It is not associated with a conference.

Acknowledgments

This study is a contribution to the PEACETIME project (http://peacetime-project.org), a joint initiative of the MERMEX and ChArMEx components supported by CNRS-INSU, IFREMER, CEA, and Météo-France as part of the programme MISTRALS coordinated by INSU. PEACETIME was endorsed as a process study by GEOTRACES. It is also a contribution to SOLAS and IMBER. We thank the captain and the crew of the RV Pourquoi Pas? for their professionalism and their work at sea. We warmly thank C. Guieu and K. Deboeufs, as coordinators of the program PEACETIME and chiefs scientists of the campaing. This work is a contribution to the "AT – POMPE BIOLOGIQUE" of the Mediterranean Institute of Oceanography (MIO). The instrument (ELEMENT XR, ThermoFisher) was supported in 2012 by European Regional Development Fund (ERDF).

Figures

Figure 1: (a) Map of the study area showing the three sub-basins (ALG, TYRR and ION) with stations' locations. The dashed line represents the zonal transect reported in Figure 2; (b) Potential temperature – salinity diagram with isopynals (kg m^{-3}) for PEACETIME profiles. Graph constructed using Ocean Data View (Schlitzer, 2002).

Figure 2: (a-e) Sections of particulate biogenic Ba (Ba_{xs}, pM), Al (pM), Sr (pM) and Ca (nM) concentrations, and % Ba_{xs} (biogenic fraction) in the upper 2000 m water column. (f) Section of PHP (ngC L^{-1} h^{-1}) is reported in the upper 500 m. Graph constructed using Ocean Data View (Schlitzer, 2002).

Figure 3: Ba_{xs} (a-c; pM) and PHP (d-f; ngC L^{-1} h^{-1}) profiles in the upper 2000 and 1000 m respectively, at long stations #Fast, #Tyrr and #Ion. The dashed grey line represents the Ba_{xs} background (Bkg) and the grey area represents the fraction for which Ba_{xs} is mostly biogenic (a-c).

Figure 4: Integrated PHP in the upper 100 m over integrated PHP in the upper 500 m versus depth-weighted average (DWA) mesopelagic Ba_{xs} (pM) over the 150-500 depth interval during PEACETIME. The same data are reported for KEOPS1 and KEOPS2 cruises (Southern Ocean; Jacquet et al., 2015) and at the PAP (NE-Atlantic) and ANTARES/EMSO-LO (NW-Mediterranean Sea) observatory sites (Jacquet et al., 2021). The blue line (R^2=0.88) represents the trend reported during KEOPS2 (Jacquet et al., 2005); it does not include encircled data points referred to as "season advancement".

Figure 5: POC remineralization fluxes (mg C m^{-2} d^{-1}) in the upper (100-500 m) and entire (100-1000 m) mesopelagic layer in the ALG, TYR and ION basins. Open squares represent primary production fluxes (mg C m^{-2} d^{-1}; Van Wambeke et al., this issue).

Tables

Table 1: Depth-weighted average (DWA) concentrations of Ba_{xs} (pM) and remineralization rates (MR; mg C m^{-2} d^{-1}) for the upper (100-500 m) and entire (100-1000 m) mesopelagic layer.

References

Ayata, S.-D., Irisson, J.-O., Aubert, A., Berline, L., Dutay, J.-C., Mayot, N., Nieblas, A.-E., D'Ortenzio, F., Palmiéri, J., Reygondeau, G., Rossi, V., and Guieu, C.: Regionalisation of the Mediterranean basin, a MERMEX synthesis, Prog. Oceanogr., 163, 7–20, https://doi.org/10.1016/j.pocean.2017.09.016, 2018.

van Beek, P., Sternberg, E., Reyss, J.-L., Souhaut, M., Robin, E., and Jeandel, C.: 228Ra/226Ra and 226Ra/Ba ratios in the Western Mediterranean Sea: Barite formation and transport in the water column, Geochim. Cosmochim. Ac., 73, 4720–4737, https://doi.org/10.1016/j.gca.2009.05.063, 2009.

Berline, L., Doglioli, A. M., Petrenko, A., Barrillon, S., Espinasse, B., Le Moigne, F. A. C., Simon-Bot, F., Thyssen, M., and Carlotti, F.: Long distance particle transport to the central Ionian Sea, Biogeosciences, 2021, 1–28, https://doi.org/10.5194/bg-2020-481, 2021.

Bertram, M. and P. Cowen, J.: Morphological and compositional evidence for biotic precipitation of marine barite, J. Mar. Res., 55, 577–593, 1997.

Boyd, P., Claustre, H., Levy, M., Siegel, D., and Weber, T.: Multi-faceted particle pumps drive carbon sequestration in the ocean, Nature, 568, 327–335, https://doi.org/10.1038/s41586-019-1098-2, 2019.

Broecker, W. S., Takahashi, T., and Takahashi, T.: Sources and flow patterns of deep-ocean waters as deduced from potential temperature, salinity, and initial phosphate concentration, J. Geophys. Res., 90, 6925–6939, https://doi.org/10.1029/JC090iC04p06925, 1985.

Buesseler, K. O. and Boyd, P. W.: Shedding light on processes that control particle export and flux attenuation in the twilight zone of the open ocean, Limnol. Oceanogr., 54, 1210–1232, https://doi.org/10.4319/lo.2009.54.4.1210, 2009.

Buesseler, K. O., Lamborg, C. H., Boyd, P. W., Lam, P. J., Trull, T. W., Bidigare, R. R., Bishop, J. K. B., Casciotti, K. L., Dehairs, F., Elskens, M., Honda, M., Karl, D. M., Siegel, D.

A., Silver, M. W., Steinberg, D. K., Valdes, J., Van Mooy, B., and Wilson, S.: Revisiting Carbon Flux Through the Ocean's Twilight Zone, Science, 316, 567–570, https://doi.org/10.1126/science.1137959, 2007.

Cardinal, D., Dehairs, F., Cattaldo, T., and André, L.: Geochemistry of suspended particles in the Subantarctic and Polar Frontal zones south of Australia: Constraints on export and advection processes, J. Geophys. Res., 106, 31637–31656, https://doi.org/10.1029/2000JC000251, 2001.

Cardinal, D., Savoye, N., Trull, T. W., André, L., Kopczynska, E. E., and Dehairs, F.: Variations of carbon remineralisation in the Southern Ocean illustrated by the Baxs proxy, Deep-Sea Res. Pt. I, 52, 355–370, https://doi.org/10.1016/j.dsr.2004.10.002, 2005.

Dehairs, F., Chesselet, R., and Jedwab, J.: Discrete suspended particles of barite and the barium cycle in the open ocean, Earth. Planet. Sc. Lett., 49, 528–550, https://doi.org/10.1016/0012-821X(80)90094-1, 1980.

Dehairs, F., Lambert, C. E., Chesselet, R., and Risler, N.: The biological production of marine suspended barite and the barium cycle in the Western Mediterranean Sea, Biogeochemistry, 4, 119–140, https://doi.org/10.1007/BF02180151, 1987.

Dehairs, F., Stroobants, N., and Goeyens, L.: Suspended barite as a tracer of biological activity in the Southern Ocean, Mar. Chem., 35, 399–410, http://dx.doi.org/10.1016/S0304-4203(09)90032-9, 1991.

Dehairs, F., Shopova, D., Ober, S., Veth, C., and Goeyens, L.: Particulate barium stocks and oxygen consumption in the Southern Ocean mesopelagic water column during spring and early summer: relationship with export production, Deep-Sea Res. Pt. II, 44, 497–516, https://doi.org/10.1016/S0967-0645(96)00072-0, 1997.

Dehairs, F., Jacquet, S., Savoye, N., Van Mooy, B. A. S., Buesseler, K. O., Bishop, J. K. B., Lamborg, C. H., Elskens, M., Baeyens, W., Boyd, P. W., Casciotti, K. L., and Monnin, C.:

Barium in twilight zone suspended matter as a potential proxy for particulate organic carbon remineralization: Results for the North Pacific, Deep-Sea Res. Pt. II, 55, 1673–1683, https://doi.org/10.1016/j.dsr2.2008.04.020, 2008.

Durrieu de Madron, X., Guieu, C., Sempéré, R., Conan, P., Cossa, D., D'Ortenzio, F., Estournel, C., Gazeau, F., Rabouille, C., Stemmann, L., Bonnet, S., Diaz, F., Koubbi, P., Radakovitch, O., Babin, M., Baklouti, M., Bancon-Montigny, C., Belviso, S., Bensoussan, N., Bonsang, B., Bouloubassi, I., Brunet, C., Cadiou, J.-F., Carlotti, F., Chami, M., Charmasson, S., Charrière, B., Dachs, J., Doxaran, D., Dutay, J.-C., Elbaz-Poulichet, F., Eléaume, M., Eyrolles, F., Fernandez, C., Fowler, S., Francour, P., Gaertner, J. C., Galzin, R., Gasparini, S., Ghiglione, J.-F., Gonzalez, J.-L., Goyet, C., Guidi, L., Guizien, K., Heimbürger, L.-E., Jacquet, S. H. M., Jeffrey, W. H., Joux, F., Le Hir, P., Leblanc, K., Lefèvre, D., Lejeusne, C., Lemé, R., Loÿe-Pilot, M.-D., Mallet, M., Méjanelle, L., Mélin, F., Mellon, C., Mérigot, B., Merle, P.-L., Migon, C., Miller, W. L., Mortier, L., Mostajir, B., Mousseau, L., Moutin, T., Para, J., Pérez, T., Petrenko, A., Poggiale, J.-C., Prieur, L., Pujo-Pay, M., Pulido-Villena, Raimbault, P., Rees, A. P., Ridame, C., Rontani, J.-F., Ruiz Pino, D., Sicre, M. A., Taillandier, V., Tamburini, C., Tanaka, T., Taupier-Letage, I., Tedetti, M., Testor, P., Thébault, H., Thouvenin, B., Touratier, F., Tronczynski, J., Ulses, C., Van Wambeke, F., Vantrepotte, V., Vaz, S., and Verney, R.: Marine ecosystems' responses to climatic and anthropogenic forcings in the Mediterranean, Prog. Oceanogr., 91, 97–166, https://doi.org/10.1016/j.pocean.2011.02.003, 2011.

Dymond, J. R., Suess, E., and Lyle, M.: Barium in deep-sea sediment: a geochemical proxy for paleoproductivity, Paleoceanography, 7, 163–181, 1992.

Ellison, S. L. R.: Eurachem/CITAC Guide CG4, Quantifying Uncertainty in Analytical Measurement, 2nd Edn., edited by: Ellison, S. L. R., Rosslein, M., and Williams, A., 120 pp., ISBN 0948926 15 5, 2000.

Ganeshram, R. S., François, R., Commeau, J., and Brown-Leger, S. L.: An experimental investigation of barite formation in seawater, Geochim. Cosmochim. Ac., 67, 2599–2605, https://doi.org/10.1016/S0016-7037(03)00164-9, 2003.

Gazeau, F., Van Wambeke, F., Marañon, E., Pérez-Lorenzo, M., Alliouane, S., Stolpe, C., Blasco, T., Leblond, N., Zäncker B., Engel A., Marie, B., Dinasquet, J., and Guieu C.: Impact of dust addition on the metabolism of Mediterranean plankton communities and carbon export under present and future conditions of pH and temperature, Biogeosciences Discuss. [preprint], https://doi.org/10.5194/bg-2021-20, in review, 2021.

Guieu, C., D'Ortenzio, F., Dulac, F., Taillandier, V., Doglioli, A., Petrenko, A., Barrillon, S., Mallet, M., Nabat, P., and Desboeufs, K.: Introduction: Process studies at the air–sea interface after atmospheric deposition in the Mediterranean Sea – objectives and strategy of the PEACETIME oceanographic campaign (May–June 2017), Biogeosciences, 17, 5563–5585, https://doi.org/10.5194/bg-17-5563-2020, 2020a.

Guieu, C., and Desboeufs, K. : PEACETIME cruise, RV Pourquoi pas?, https://doi.org/10.17600/17000300, 2017.

Guieu, C., Desboeufs, K., Albani, S., et al.: Biogeochemical dataset collected during the PEACETIME cruise, available at: https://www.seanoe.org/data/00645/75747/, 2020b.

Hainbucher, D., Rubino, A., Cardin, V., Tanhua, T., Schroeder, K., and Bensi, M.: Hydrographic situation during cruise M84/3 and P414 (spring 2011) in the Mediterranean Sea, Ocean Sci., 10, 669–682, https://doi.org/10.5194/os-10-669-2014, 2014.

Henson, S. A., Sanders, R., Madsen, E., Morris, P. J., Le Moigne, F., and Quartly, G. D.: A reduced estimate of the strength of the ocean's biological carbon pump, Geophys. Res. Lett., 38, L04606, https://doi.org/10.1029/2011GL046735, 2011.

IPCC: 5th Assessment Report (AR5) Climate Change 2013, Working Group 1, January 2014.

a mis en forme : Anglais (E.U.)

Jacquet, S. H. M., Dehairs, F., Elskens, M., Savoye, N., and Cardinal, D.: Barium cycling along WOCE SR3 line in the Southern Ocean, Mar. Chem., 106, 33–45, https://doi.org/10.1016/j.marchem.2006.06.007, 2007a.

Jacquet, S. H. M., Henjes, J., Dehairs, F., Worobiec, A., Savoye, N., and Cardinal, D.: Particulate Ba-barite and acantharians in the Southern Ocean during the European Iron Fertilization Experiment (EIFEX), J. Geophys. Res., 112, https://doi.org/10.1029/2006JG000394, 2007b.

Jacquet, S. H. M., Savoye, N., Dehairs, F., Strass, V. H., and Cardinal, D.: Mesopelagic carbon remineralization during the European Iron Fertilization Experiment, Global Biogeochem. Cycles, 22, GB1023, https://doi.org/10.1029/2006GB002902, 2008a.

Jacquet, S. H. M., Dehairs, F., Savoye, N., Obernosterer, I., Christaki, U., Monnin, C., and Cardinal, D.: Mesopelagic organic carbon remineralization in the Kerguelen Plateau region tracked by biogenic particulate Ba, Deep-Sea Res. Pt. II, 55, 868–879, https://doi.org/10.1016/j.dsr2.2007.12.038, 2008b.

Jacquet, S. H. M., Dehairs, F., Dumont, I., Becquevort, S., Cavagna, A.-J., and Cardinal, D.: Twilight zone organic carbon remineralization in the Polar Front Zone and Subantarctic Zone south of Tasmania, Deep-Sea Res. Pt. II, 58, 2222–2234, https://doi.org/10.1016/j.dsr2.2011.05.029, 2011.

Jacquet, S. H. M., Dehairs, F., Lefèvre, D., Cavagna, A. J., Planchon, F., Christaki, U., Monin, L., André, L., Closset, I., and Cardinal, D.: Early spring mesopelagic carbon remineralization and transfer efficiency in the naturally iron-fertilized Kerguelen area, Biogeosciences, 12, 1713–1731, https://doi.org/10.5194/bg-12-1713-2015, 2015.

Jacquet, S. H. M., Monnin, C., Riou, V., Jullion, L., and Tanhua, T.: A high resolution and quasi-zonal transect of dissolved Ba in the Mediterranean Sea, Mar. Chem., 178, 1–7, https://doi.org/10.1016/j.marchem.2015.12.001, 2016.

Jacquet, S. H. M., Lefèvre, D., Tamburini, C., Garel, M., Le Moigne, F. A. C., Bhairy, N., and Guasco, S.: On the barium–oxygen consumption relationship in the Mediterranean Sea: implications for mesopelagic marine snow remineralization, Biogeosciences, 18, 2205–2212, https://doi.org/10.5194/bg-18-2205-2021, 2021.

Jullion, L., Jacquet, S. H. M., and Tanhua, T.: Untangling biogeochemical processes from the impact of ocean circulation: First insight on the Mediterranean dissolved barium dynamics, Global Biogeochem. Cycles, 31, 1256–1270, https://doi.org/10.1002/2016GB005489, 2017.

Kirchman, D. L.: Leucine incorporation as a measure of biomass production by heterotrophic bacteria, in: Handbooks of methods in aquatic microbial ecology,, edited by: Kemp, P. F., Sherr, B. F., Sherr, E. B., and Cole, J. J., Lewis Publishers, Boca Raton, Ann Arbor, London, Tokyo, 509–512, 1993.

Kwon, E. Y., Primeau, F., and Sarmiento, J. L.: The impact of remineralization depth on the air–sea carbon balance, Nat. Geosci., 2, 630–635, https://doi.org/10.1038/ngeo612, 2009.

Lemaitre, N., Planquette, H., Planchon, F., Sarthou, G., Jacquet, S., García-Ibáñez, M. I., Gourain, A., Cheize, M., Monin, L., André, L., Laha, P., Terryn, H., and Dehairs, F.: Particulate barium tracing of significant mesopelagic carbon remineralisation in the North Atlantic, Biogeosciences, 15, 2289–2307, https://doi.org/10.5194/bg-15-2289-2018, 2018.

López-Sandoval, D. C., Fernández, A., and Marañón, E.: Dissolved and particulate primary production along a longitudinal gradient in the Mediterranean Sea, Biogeosciences, 8, 815–825, https://doi.org/10.5194/bg-8-815-2011, 2011.

Luna, G. M., Bianchelli, S., Decembrini, F., De Domenico, E., Danovaro, R., and Dell'Anno, A.: The dark portion of the Mediterranean Sea is a bioreactor of organic matter cycling, Global Biogeochem. Cycles, 26, GB2017, https://doi.org/10.1029/2011GB004168, 2012.

Malanotte-Rizzoli, P., Artale, V., Borzelli-Eusebi, G. L., Brenner, S., Crise, A., Gacic, M., Kress, N., Marullo, S., Ribera d'Alcalà, M., Sofianos, S., Tanhua, T., Theocharis, A., Alvarez, M., Ashkenazy, Y., Bergamasco, A., Cardin, V., Carniel, S., Civitarese, G., D'Ortenzio, F., Font, J., Garcia-Ladona, E., Garcia-Lafuente, J. M., Gogou, A., Gregoire, M., Hainbucher, D., Kontoyannis, H., Kovacevic, V., Kraskapoulou, E., Kroskos, G., Incarbona, A., Mazzocchi, M. G., Orlic, M., Ozsoy, E., Pascual, A., Poulain, P.-M., Roether, W., Rubino, A., Schroeder, K., Siokou-Frangou, J., Souvermezoglou, E., Sprovieri, M., Tintoré, J., and Triantafyllou, G.: Physical forcing and physical/biochemical variability of the Mediterranean Sea: a review of unresolved issues and directions for future research, Ocean Sci., 10, 281–322, https://doi.org/10.5194/os-10-281-2014, 2014.

Martin, J. H., and G. A. Knauer (1973), Elemental composition of plankton, Geochim. Cosmochim. Acta, 37(7), 1639– 1653.

Martin, J. H., Knauer, G. A., Karl, D. M., and Broenkow, W. W.: VERTEX: carbon cycling in the northeast Pacific, Deep-Sea Res., 34, 267–285, http://dx.doi.org/10.1016/0198-0149(87)90086-0, 1987.

Monnin, C. and Cividini, D.: The saturation state of the world's ocean with respect to (Ba,Sr)SO4 solid solutions, Geochim. Cosmochim. Ac., 70, 3290–3298, https://doi.org/10.1016/j.gca.2006.04.002, 2006.

Moutin, T. and Raimbault, P.: Primary production, carbon export and nutrients availability in western and eastern Mediterranean Sea in early summer 1996 (MINOS cruise), J. Marine Syst., 33–34, 273–288, https://doi.org/10.1016/S0924-7963(02)00062-3, 2002.

Pabortsava, K., Lampitt, R. S., Benson, J., Crowe, C., McLachlan, R., Le Moigne, F. A. C., Mark Moore, C., Pebody, C., Provost, P., Rees, A. P., Tilstone, G. H., and Woodward, E. M. S.: Carbon sequestration in the deep Atlantic enhanced by Saharan dust, Nature Geoscience, 10, 189–194, https://doi.org/10.1038/ngeo2899, 2017.

Planchon, F., Cavagna, A.-J., Cardinal, D., André, L., and Dehairs, F.: Late summer particulate organic carbon export and twilight zone remineralisation in the Atlantic sector of the Southern Ocean, Biogeosciences, 10, 803–820, https://doi.org/10.5194/bg-10-803-2013, 2013.

Pujo-Pay, M., Conan, P., Oriol, L., Cornet-Barthaux, V., Falco, C., Ghiglione, J.-F., Goyet, C., Moutin, T., and Prieur, L.: Integrated survey of elemental stoichiometry (C, N, P) from the western to eastern Mediterranean Sea, Biogeosciences, 8, 883–899, https://doi.org/10.5194/bg-8-883-2011, 2011.

Reygondeau, G., Guieu, C., Benedetti, F., Irisson, J.-O., Ayata, S.-D., Gasparini, S., and Koubbi, P.: Biogeochemical regions of the Mediterranean Sea: An objective multidimensional and multivariate environmental approach, Prog. Oceanogr., 151, 138–148, http://dx.doi.org/10.1016/j.pocean.2016.11.001, 2017.

Sanchez-Vidal, A., Collier, R. W., Calafat, A., Fabres, J., and Canals, M.: Particulate barium fluxes on the continental margin: a study from the Alboran Sea (Western Mediterranean), Mar. Chem., 93, 105–117, https://doi.org/10.1016/j.marchem.2004.07.004, 2005.

Santinelli, C., Nannicini, L., and Seritti, A.: DOC dynamics in the meso and bathypelagic layers of the Mediterranean Sea, Deep-Sea Res. Pt. II, 57, 1446–1459, https://doi.org/10.1016/j.dsr2.2010.02.014, 2010.

Schlitzer, R.: Ocean Data View, GEO/ODV, available at: http://www.awi-bremerhaven.de/ (last access: 2 March 2021), 2002.

Simon, M. and Azam, F.: Protein content and protein synthesis rates of planktonic marine bacteria, Mar. Ecol. Prog. Ser., 51, 201–213, 1989.

Stabholz, M., Durrieu de Madron, X., Canals, M., Khripounoff, A., Taupier-Letage, I., Testor, P., Heussner, S., Kerhervé, P., Delsaut, N., Houpert, L., Lastras, G., and Dennielou, B.: Impact of open-ocean convection on particle fluxes and sediment dynamics in the deep margin of the Gulf of Lions, Biogeosciences, 10, 1097–1116, https://doi.org/10.5194/bg-10-1097-2013, 2013.

Stange, P., Bach, L. T., Le Moigne, F. A. C., Taucher, J., Boxhammer, T., and Riebesell, U.: Quantifying the time lag between organic matter production and export in the surface ocean: Implications for estimates of export efficiency, Geophys. Res. Lett., 44, 268–276, https://doi.org/10.1002/2016GL070875, 2017.

Sternberg, E., Jeandel, C., Miquel, J.-C., Gasser, B., Souhaut, M., Arraes-Mescoff, R., and Francois, R.: Particulate barium fluxes and export production in the northwestern Mediterranean, Mar. Chem., 105, 281–295, https://doi.org/10.1016/j.marchem.2007.03.003, 2007.

Sternberg, E., Jeandel, C., Robin, E., and Souhaut, M.: Seasonal cycle of suspended barite in the mediterranean sea, Geochim. Cosmochim. Ac., 72, 4020–4034, https://doi.org/10.1016/j.gca.2008.05.043, 2008.

Stroobants, N., Dehairs, F., Goeyens, L., Vanderheijden, N., and Van Grieken, R.: Barite formation in the Southern Ocean water column, Mar. Chem., 35, 411–421, https://doi.org/10.1016/S0304-4203(09)90033-0, 1991.

Tamburini, C., Garcin, J., Ragot, M., and Bianchi, A.: Biopolymer hydrolysis and bacterial production under ambient hydrostatic pressure through a 2000m water column in the NW Mediterranean, Deep-Sea Res. Pt. I, 49, 2109–2123, https://doi.org/10.1016/S0967-0645(02)00030-9, 2002.

Tamburini, C., Boutrif, M., Garel, M., Colwell, R. R., and Deming, J. W.: Prokaryotic responses to hydrostatic pressure in the ocean – a review, Environ. Microbiol., 15, 1262–1274, https://doi.org/10.1111/1462-2920.12084, 2013.

Tanhua, T., Hainbucher, D., Cardin, V., Álvarez, M., Civitarese, G., McNichol, A. P., and Key, R. M.: Repeat hydrography in the Mediterranean Sea, data from the <i>Meteor</i> cruise 84/3 in 2011, Earth Syst. Sci. Data, 5, 289–294, https://doi.org/10.5194/essd-5-289-2013, 2013a.

Tanhua, T., Hainbucher, D., Schroeder, K., Cardin, V., Álvarez, M., and Civitarese, G.: The Mediterranean Sea system: a review and an introduction to the special issue, Ocean Sci., 9, 789–803, https://doi.org/10.5194/os-9-789-2013, 2013b.

Taylor, S. R. and McLennan, S. M.: The continental crust: its composition and evolution, Blackwell Scientific Publications, USA, 312 pp., 1985.

Van Wambeke, F., Taillandier, V., Deboeufs, K., Pulido-Villena, E., Dinasquet, J., Engel, A., Marañón, E., Ridame, C., and Guieu, C.: Influence of atmospheric deposition on biogeochemical cycles in an oligotrophic ocean system, Biogeosciences, 2020, 1–51, https://doi.org/10.5194/bg-2020-411, 2020.

Figure 1

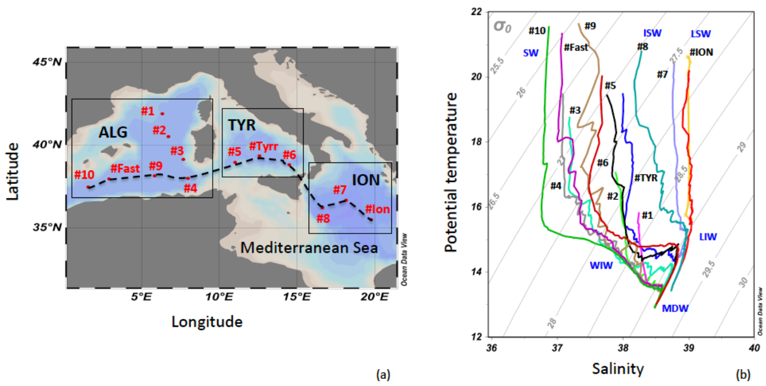
45°N
40°N
35°N
5°E
10°E
15°E
20°E
Latitude
Longitude
ALG
TYR
ION
Mediterranean Sea
#1
#2
#3
#4
#5
#6
#7
#8
#9
#10
#Fast
#Tyrr
#Ion
Ocean Data View
(a)
Potential temperature
Salinity
σ0
SW
ISW
LSW
LIW
WIW
MDW
#ION
#TYR
(b)

Figure 2

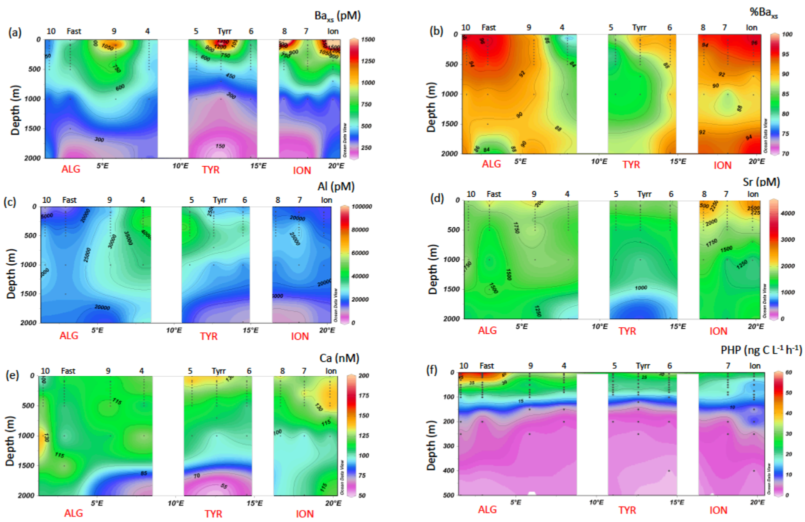
(a)
Ba$_{xs}$ (pM)
(b)
%Ba$_{xs}$
(c)
Al (pM)
(d)
Sr (pM)
(e)
Ca (nM)
(f)
PHP (ng C L^{-1} h^{-1})
Depth (m)
10
Fast
9
4
5
Tyrr
6
8
7
Ion
ALG
TYR
ION
5°E
10°E
15°E
20°E

Figure 3

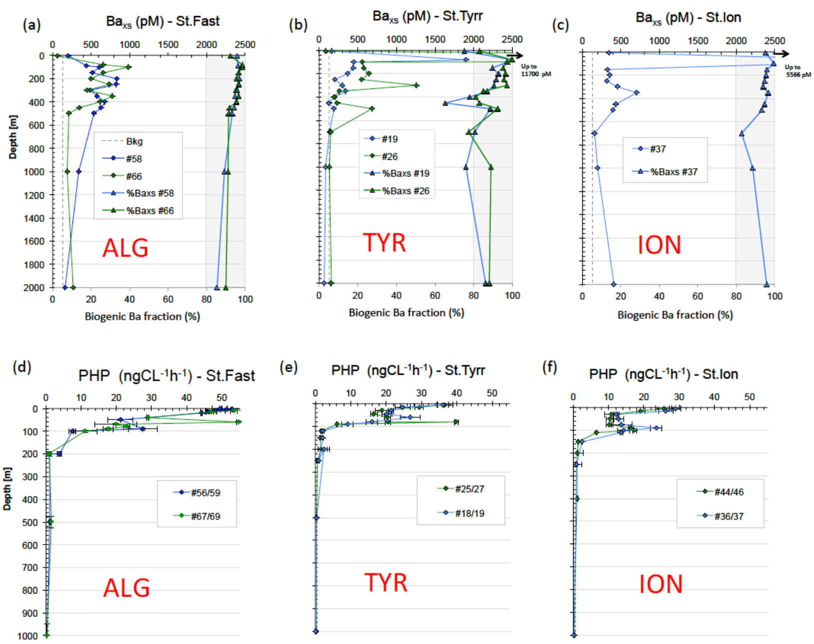
(a)
Ba_{xs} (pM) - St.Fast
Depth [m]
Bkg
#58
#66
%Baxs #58
%Baxs #66
ALG
Biogenic Ba fraction (%)
(b)
Ba_{xs} (pM) - St.Tyrr
Up to 11700 pM
#19
#26
%Baxs #19
%Baxs #26
TYR
Biogenic Ba fraction (%)
(c)
Ba_{xs} (pM) - St.Ion
Up to 5566 pM
#37
%Baxs #37
ION
Biogenic Ba fraction (%)
(d)
PHP (ngCL^{-1}h^{-1}) - St.Fast
Depth [m]
#56/59
#67/69
ALG
(e)
PHP (ngCL^{-1}h^{-1}) - St.Tyrr
#25/27
#18/19
TYR
(f)
PHP (ngCL^{-1}h^{-1}) - St.Ion
#44/46
#36/37
ION

Figure 4

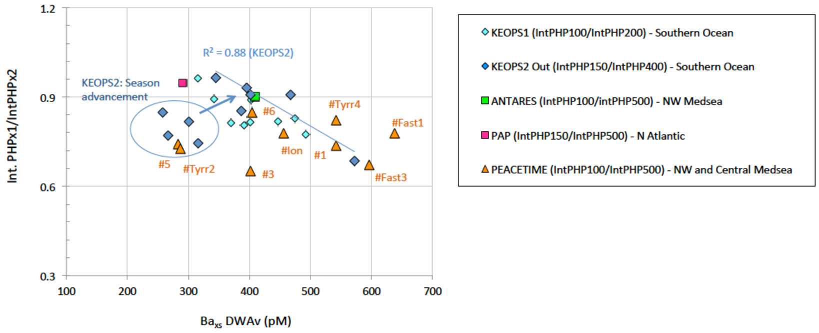

1.2
0.9
0.6
0.3
100
200
300
400
500
600
700
Int. PHPx1/IntPHPx2
Ba$_{xs}$ DWAv (pM)
R² = 0.88 (KEOPS2)
KEOPS2: Season advancement
#Tyrr4
#6
#Fast1
#Ion
#1
#5
#Tyrr2
#3
#Fast3
KEOPS1 (IntPHP100/IntPHP200) - Southern Ocean
KEOPS2 Out (IntPHP150/IntPHP400) - Southern Ocean
ANTARES (IntPHP100/intPHP500) - NW Medsea
PAP (IntPHP150/IntPHP500) - N Atlantic
PEACETIME (IntPHP100/IntPHP500) - NW and Central Medsea

Figure 5

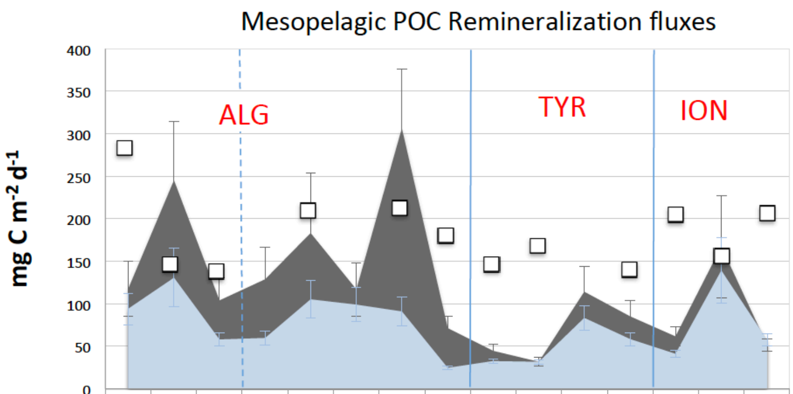

	1	2	3	10	Fast1	Fast3	9	4	5	Tyrr2	Tyrr4	6	8	7	Ion1
100-1000m	117	245	104	129	183	117	306	71	45	32	114	85	62	167	52
100-500m	94	131	58	60	105	99	91	25	32	32	84	58	41	139	58

Table 1

Basin	Station #	Mesopelagic layer	DWAv Ba_{xs} [pM]	MR [mg C m^{-2} d^{-1}]	Stnd error (%)
Algero-Provençal	1	upper	542	94	20
	1	entire	374	117	27
	2	upper	717	131	26
	2	entire	645	245	28
	3	upper	402	58	13
	3	entire	353	104	25
	4	upper	243	25	8
	4	entire	281	71	20
	9	upper	981	91	19
	9	entire	979	306	23
	Fast1	upper	638	105	21
	Fast1	entire	527	183	38
	Fast3	upper	596	99	20
	Fast3	entire	381	117	27
	10	upper	418	60	13
	10	entire	410	129	29
Tyrrhenian	5	upper	283	32	9
	5	entire	226	45	17
	Tyrr2	upper	284	32	9
	Tyrr2	entire	200	32	15
	Tyrr4	upper	542	84	17
	Tyrr4	entire	380	114	26
	6	upper	404	58	13
	6	entire	313	85	22
Ionian	7	upper	769	139	28
	7	entire	485	167	36
	ION	upper	456	58	13
	ION	entire	315	52	13
	8	upper	363	41	10
	8	entire	273	62	18